

ON PAIR PRODUCTION OF SCALAR TOP QUARKS IN e^+e^- COLLISIONS AT ILC AND A POSSIBILITY OF THEIR MASS RECONSTRUCTION

A. Bartl^{a,b}, W. Majerotto^c,
K. Mönig^d, A.N. Skachkova^e, N.B. Skachkov^e

^a *University of Vienna, Faculty of Physics, 1090 Vienna, Boltzmannngasse 5, Austria.*

^b *AHEP Group, Instituto de Física Corpuscular - C.S.I.C., Universidad de Valencia, Edificio Institutos de Investigacion, Apt. 22085, E-46071 Valencia, Spain.*

^c *Institute for High Energy Physics (HEPHY Vienna), Nikolsdorfergasse 18, A-1050 Vienna, Austria.*

^d *DESY, Platanenallee 6, D-15738 Zeuthen, Germany.*

^e *JINR, Joliot-Curie 6, 141980 Dubna, Moscow region, Russia.*

Abstract

We study pair production of scalar top quarks (stop, \tilde{t}_1) in e^+e^- collisions with the subsequent decay of the top squarks into b -quarks and charginos $\tilde{t}_1 \rightarrow b\tilde{\chi}_1^\pm$. We simulate this process by using PYTHIA6.4 for the beam energy $2E_b = \sqrt{s} = 350, 400, 500, 800, 1000$ GeV. A set of criteria for physical variables is proposed, which provides good separation of stop signal events from top quark pair production being the main background. These criteria allow us to reconstruct the mass of the top squark with an integrated luminosity of 1000 fb^{-1} provided that the neutralino mass is known.

1 Introduction.

The scalar top quark, the bosonic partner of the top quark, has attracted much attention as it is expected to be the lightest colored supersymmetric (SUSY) particle. \tilde{t}_L and \tilde{t}_R , the supersymmetric partners of the left-handed and right-handed top quarks, mix and the resulting two mass eigenstates \tilde{t}_1 and \tilde{t}_2 , can have a large mass splitting. It is even possible that the lighter eigenstate \tilde{t}_1 could be lighter than the top quark itself [1].

Searches for top squarks which were performed at LEP and Tevatron [2], have shown that the mass of the stop is higher than 141 GeV for a mass difference between the stop and the lightest neutralino of about 50-70 GeV. These searches will continue at LHC and ILC [3], [4].

In the following we study the reaction ¹

$$e^+ + e^- \rightarrow \tilde{t}_1 + \tilde{t}_1^* . \quad (1)$$

¹More details about this study can be found in [5]. The analogous analysis in the photon-photon channel was made in [6].

Among the possible \tilde{t}_1 -decay channels within the MSSM (see [7] for details), we focus on the decay $\tilde{t}_1 \rightarrow b\tilde{\chi}_1^\pm$ followed by the two-body chargino decay $\tilde{\chi}_1^\pm \rightarrow \tilde{\chi}_1^0 W^\pm$, where one of the W 's decays hadronically, $W \rightarrow q_i \bar{q}_j$, and the other one leptonically, $W \rightarrow \mu \nu_\mu$ [8]². The final state of this signal process, shown in the left-hand plot of Fig.1, contains two b -jets and two (or more) jets (originating from the decay of one W boson), a hard muon plus a neutrino (from the decay of the other W) and two neutralinos:

$$e^+e^- \rightarrow \tilde{t}_1\tilde{t}_1 \rightarrow b\bar{b}\tilde{\chi}_1^+\tilde{\chi}_1^- \rightarrow b\bar{b}W^+W^-\tilde{\chi}_1^0\tilde{\chi}_1^0 \rightarrow b\bar{b}q_i\bar{q}_j\mu\nu_\mu\tilde{\chi}_1^0\tilde{\chi}_1^0. \quad (2)$$

The main background process is top quark pair production with the subsequent decay $t \rightarrow bW^\pm$ (for W 's we use the same decay channels as in the stop case):

$$e^+e^- \rightarrow t\bar{t} \rightarrow b\bar{b}W^+W^- \rightarrow b\bar{b}q_i\bar{q}_j\mu\nu_\mu. \quad (3)$$

The only difference between the final states of stop and top production (shown in the right diagram of Fig.1) is that in stop pair production there are two neutralinos which are undetectable. Thus, both processes have the same signature: two b -jets, two jets from W decay and a muon. In the present paper we consider only top pair production as background. The

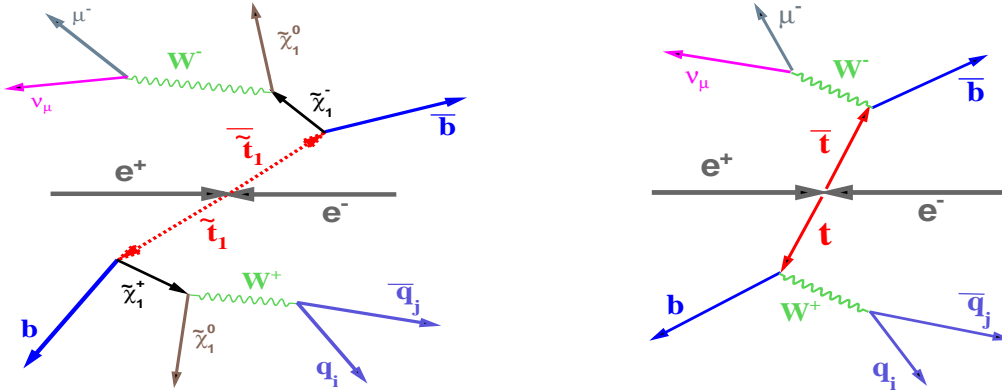


Figure 1: Left is the stop signal event diagram, Right is the top background diagram.

analysis of the processes (2) and (3) is done on the basis of Monte Carlo samples of the corresponding events generated by the two programs PYTHIA6.4 [10] and CIRCE1 [11]. The program CIRCE1 is used for the parameterization of the beam spectra involved in processes (1) and (3) to account for the effects of beamstrahlung. The energy of the beams was chosen as $2E_b = \sqrt{s} = 350, 400, 500, 800, 1000$ GeV.

In Section 2 we give the set of MSSM parameters used in our study.

In Section 3 we discuss some general characteristics of the signal process $e^+e^- \rightarrow \tilde{t}_1\tilde{t}_1$ and the main background $e^+e^- \rightarrow t\bar{t}$. First we show the result of taking into account beam interaction effects like beamstrahlung and others which are simulated with CIRCE1 [11]. The distributions for a set of physical variables, which are measurable in the final state of the process (2), are given for the case of a beam energy $\sqrt{s} = 500$ GeV and integrated luminosity of $1000 fb^{-1}$. These variables include hadronic jets from W -decay as well as b -jets produced in stop decays. We always compare them in detail with those of top pair production.

In Section 4 we propose three cuts which allow a good separation of signal stop events and background top events. The number of stop events that have passed these cuts and the values of the corresponding efficiencies are given. We show that the invariant mass of one

²The process $e^+e^- \rightarrow \tilde{t}_1 + \tilde{t}_1$ with the subsequent decay $\tilde{t}_1 \rightarrow c\tilde{\chi}_1^0$ was considered in [9].

b -jet and the other two *non* – b -jets (from W decay) allows one to reconstruct the mass of the scalar top quark provided that the neutralino mass is known. The impact of the proposed cuts on the values of the cross sections of stop and top pair productions are shown together with the values of signal-to-background ratios (S/B). We have also considered a cut which allows to separate a signal muon from W decay and fake muons appearing due to decays of other particles in the same stop production event.

Section 5 contains some conclusions.

2 MSSM parameters and cross section.

The scalar top quark system is described by the mass matrix (in the $\tilde{t}_L - \tilde{t}_R$ basis) [1], [12]

$$\begin{pmatrix} M_{\tilde{t}_{LL}}^2 & M_{\tilde{t}_{LR}}^2 \\ M_{\tilde{t}_{RL}}^2 & M_{\tilde{t}_{RR}}^2 \end{pmatrix} \quad (4)$$

with

$$M_{\tilde{t}_{LL}}^2 = M_{\tilde{Q}}^2 + \left(\frac{1}{2} - \frac{2}{3}\sin^2\Theta_W\right)\cos 2\beta M_Z^2 + M_t^2, \quad (5)$$

$$M_{\tilde{t}_{RR}}^2 = M_{\tilde{U}}^2 + \frac{2}{3}\sin^2\Theta_W\cos 2\beta M_Z^2 + M_t^2, \quad (6)$$

$$M_{\tilde{t}_{RL}}^2 = (M_{\tilde{t}_{LR}}^2)^* = M_t(A_t - \mu^*\cot\beta). \quad (7)$$

The mass eigenvalues are given by

$$M_{\tilde{t}_{1,2}}^2 = \frac{1}{2} \left[(M_{\tilde{t}_{LL}}^2 + M_{\tilde{t}_{RR}}^2) \mp \sqrt{(M_{\tilde{t}_{LL}}^2 - M_{\tilde{t}_{RR}}^2)^2 + 4|M_{\tilde{t}_{LR}}^2|^2} \right] \quad (8)$$

with the mixing angle

$$\cos\theta_{\tilde{t}} = \frac{-M_{\tilde{t}_{LR}}^2}{\sqrt{|M_{\tilde{t}_{LR}}^2|^2 + (M_{\tilde{t}_{LL}}^2 - M_{\tilde{t}_{RR}}^2)^2}}, \quad (9)$$

$$\sin\theta_{\tilde{t}} = \frac{M_{\tilde{t}_{LL}}^2 - M_{\tilde{t}_{RR}}^2}{\sqrt{|M_{\tilde{t}_{LR}}^2|^2 + (M_{\tilde{t}_{LL}}^2 - M_{\tilde{t}_{RR}}^2)^2}}. \quad (10)$$

In the following we will consider a particular choice of the MSSM parameters that are defined, in the notations of PYTHIA6.4, in the following way:

$$M_{\tilde{Q}} = 270 \text{ GeV}; \quad M_{\tilde{U}} = 270 \text{ GeV}; \quad A_t = -500 \text{ GeV (top trilinear coupling);}$$

$$\tan\beta = 5; \quad \mu = -370 \text{ GeV}; \quad M_1 = 80 \text{ GeV}; \quad M_2 = 160 \text{ GeV}.$$

Note that in PYTHIA6.4 $M_{\tilde{Q}}$ corresponds to $M_{\tilde{t}_L}$ (left squark mass for the third generation) and $M_{\tilde{U}}$ corresponds to $M_{\tilde{t}_R}$. These parameters give $M_{\tilde{t}_1} = 167.9 \text{ GeV}$, $M_{\tilde{\chi}_1^+} = 159.2 \text{ GeV}$ and $M_{\tilde{\chi}_1^0} = 80.9 \text{ GeV}$. This value of $M_{\tilde{t}_1}$ is rather close to the mass of the top quark $M_{top} = 170.9 \pm 1.8 \text{ GeV}$ [13]. Therefore one expects a rather large contribution from the top background, which means that the choice of this value of the stop mass makes the analysis most difficult. Finding a suitable set of cuts separating stop and top events is crucial.

In general, the cross section for stop pair production at a fixed energy depends on the mass of the stop quark and the mixing angle $\theta_{\tilde{t}}$. Since the couplings of the Z^0 to the left and right components of the stop are different, the cross sections depend significantly on the

beam polarizations (see [7], [8], [14]). By choosing appropriate longitudinal beam polarizations it is possible to enhance the cross sections. For example, for an electron beam with 90% left polarization the cross section would be larger than the unpolarized cross section by approximately 40%, for $\cos \theta_{\bar{t}} = -0.81$ corresponding to the parameters given above. If in addition the positron beam has 60% right polarization, then the cross section is enhanced by approximately a factor of 2 compared to the unpolarized cross section. We note that a rather precise determination of the stop mixing angle $\theta_{\bar{t}}$ is possible by measuring the left-right asymmetry. The cross section for top pair production has also a characteristic dependence on the beam polarizations [14]. For example, the polarization of both beams leads to an increase of the cross section by about a factor of 1.5.

3 Distributions of kinematic variables in stop and top production.

In this Section we present some plots of distributions for different physical variables based on $5 \cdot 10^4$ stop pair production events generated by PYTHIA6.4 and CIRCE1 weighted with the electron-positron luminosity. Analogous plots are also given for 10^6 generated background top events.

The ILC is a 200-500 GeV center-of-mass high luminosity (a peak luminosity of $\sim 2 \cdot 10^{34} \text{cm}^{-2} \text{s}^{-1}$) linear electron-positron collider with a possible upgrade to 1 TeV in the second phase. According to [3] a total luminosity of 500fb^{-1} is foreseen within the first four years of operation and 1000fb^{-1} during the first phase of operation at 500 GeV. A first run at $\sqrt{s} = 500 \text{GeV}$ will get a first measurement of the particle masses to optimize the threshold scan [4].

Fig.2 a) demonstrates the total energy spectrum of the electron and positron beams, which is expected at $\sqrt{s} = 500 \text{GeV}$ after taking into account beamstrahlung and other beam interaction effects (see, for instance [15]). Fig.2 b) shows the correlations of the beam fractions $y_i = E^i/E_{beam}^i$ ($i=e^+, e^-$) of the colliding electron and positron beams.

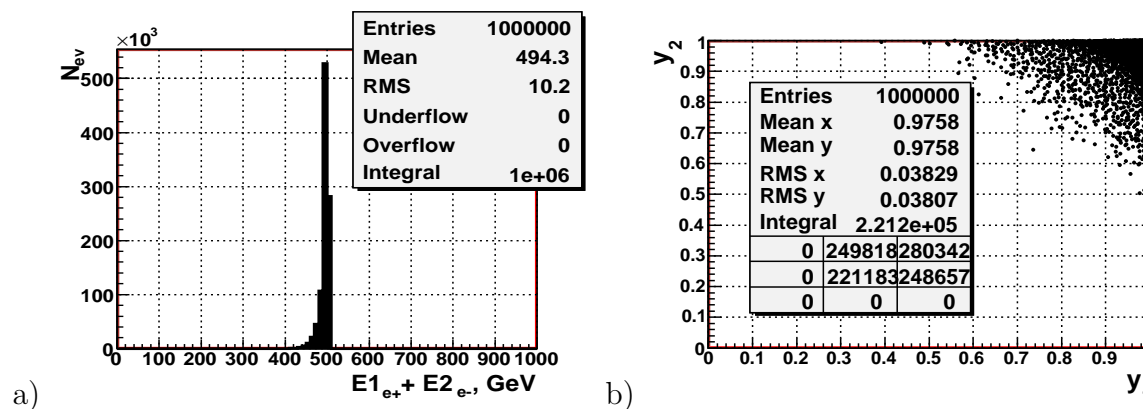


Figure 2: a) total beam energy spectrum, b) beam fractions correlations

To find the jets we used the subroutine PYCLUS of PYTHIA with the distance measure used in the "Durham algorithm". The parameters of this jetfinder are chosen such that the number of jets is exactly four. Technically, b -jets are defined as jets that contain at least one B-hadron. Their decay may be identified by the presence of a secondary vertex [16].

Let us also mention that separate stop and top event samples were generated without and with cuts. This shows the effect of the cuts.

3.1 Global jet variables.

In this subsection we present some plots that were obtained without cuts. In addition to the two b -jets there are also, according to the decay chain (2), two jets due to the decay of one W boson into two quarks $W \rightarrow q_i + \bar{q}_j$ (see Fig.1). It is well known that the characteristics of individual jets depend on the choice of the jet finder and its parameters. This dependence may result in some redistribution of energy between jets. To diminish these effects we use three physical variables which characterise the physical system composed of b -jets and the jets produced by quarks in the W decay. The simulation has shown that the effect of energy redistribution between jets is partially compensated in multijet systems.

For this reason we consider first the invariant mass of all four jets produced in the events which is the modulus of the vectorial sum of the 4-momenta P_{jet}^j ³

$$M_{inv}(Alljets) = \sqrt{(\sum_{j=1,2,3,4} P_{jet}^j)^2}. \quad (11)$$

The distribution of this invariant mass is shown in Fig.3. Plot **a)** shows the results for stop pair production while the plot **b)** is for top pair production. In Fig.3 and the following figures the vertical axis shows the number of stop and top events that may be expected for the integrated luminosity of 1000 fb^{-1} . Taking the integral of the distributions one can get the total number of events expected for the taken integral luminosity. These numbers are shown as "Integral" values in the Figures. One sees that for the chosen luminosity the number of the produced background top events (35 930) is about 15 times higher than the number of stop events (2373). It gives a signal-to-background ratio $S/B = 0.066$.

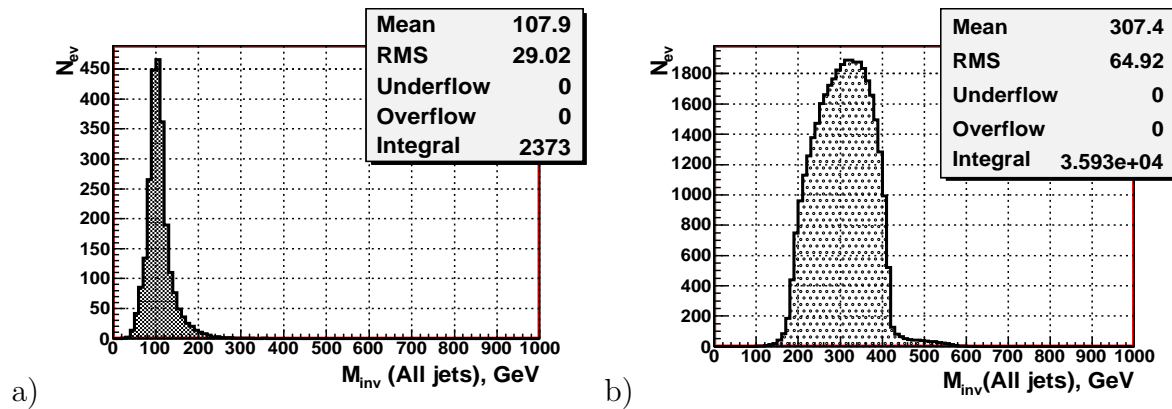


Figure 3: *Distribution of events versus the reconstructed invariant mass of all jets $M_{inv}(Alljets)$. a) stop pair production, b) top pair production.*

Plot **a)** of Fig.3 shows that the mean value of $M_{inv}(Alljets)$ is about three times lower in stop production than in top case, plot **b)** of Fig.3. Therefore, a rather soft cut like $M_{inv}(Alljets) \leq 160 \text{ GeV}$, will strongly suppress the top background and save the bulk of signal stop events. Another useful variable that can also be used for the separation of the signal and the background is the "missing" mass (we use $\sqrt{s} = 500 \text{ GeV}$)

$$M_{miss} = \sqrt{(\sqrt{s_{ee}} - (\sum_{j=1,2,3,4} E_{jet}^j + E_{\mu}))^2 - (\sum_{j=1,2,3,4} \mathbf{P}_{jet}^j + \mathbf{P}_{\mu})^2}. \quad (12)$$

This variable takes into account the contribution of those particles that cannot be registered in the detector (neutrinos and neutralinos). The distributions of this invariant "missing" mass

³ $P = (P_0, \mathbf{P})$, $P_0 = E_p$. We denote \mathbf{P}_{jet}^j as the 3-momentum of the jet j : $(\mathbf{P}^j)_i = (P^j)_i$, $(i = 1, 2, 3)$. The sum in (11) is over all four jets ($j = 1, 2, 3, 4$).

are given in Fig.4. Plot **a)** shows the results for stop pair production, while the plot **b)** is for top pair production. As seen from these plots, the cut $M_{miss} \geq 250$ GeV will also allow us to get rid of most of the background events.

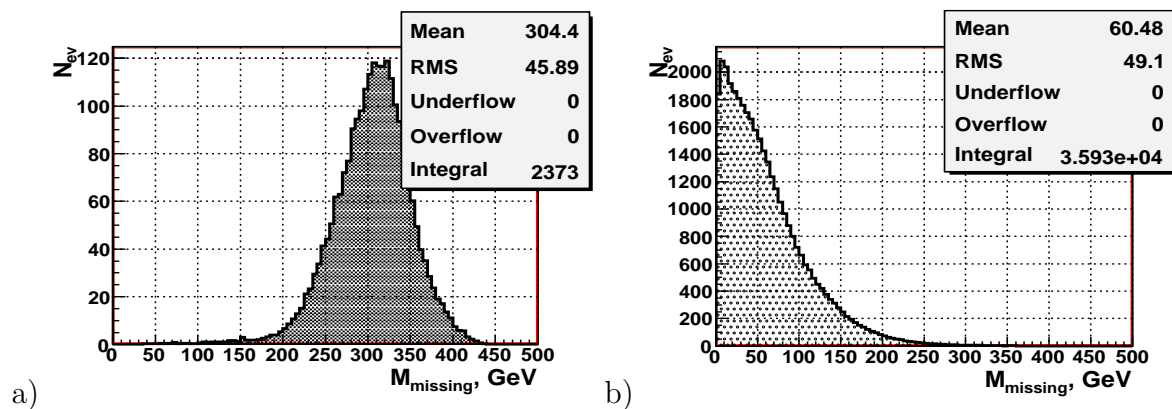


Figure 4: *Distribution of number of events versus the missing mass variable. a) stop pair production, b) top pair production.*

The third variable of interest is the invariant mass $M_{inv}(b\text{-jet}, JETS_W)$

$$\begin{aligned}
 M_{inv}(b - jet, JETS_W) &\equiv M_{inv}[b - jet + (all - non - b - jets)] = \\
 &= \sqrt{(P_{b-jet} + P_{all-non-b-jets})^2}, \quad (13)
 \end{aligned}$$

which is constructed as the modulus of the vectorial sum of the 4-momentum P_{b-jet} of the b -jet, plus the total 4-momentum of "all-non- b -jets" system stemming from the W decay ($P_{all-non-b-jets} = P_{jet1W} + P_{jet2W}$, as there are only two jets allowed to be produced in W decay). More precisely, if the signal event contains a μ^- as the signal muon, we have to take the b -jet (\bar{b} -jet would be in the case of μ^+ signal muon) (see Fig.1). This is only possible if one can discriminate between b - and \bar{b} -jets experimentally. Methods of experimental determination of the charge of the b -jet (\bar{b} -jet) were developed in [18]. In this paper we do not use any b -tagging procedure. The PYTHIA information on the quark flavour is taken for choosing the b and \bar{b} jets.

In the top case the invariant mass $M_{inv}(b, 2 quarks_W)$ of the system composed of a b -quark and two quarks from W decay should reproduce the mass of their parent top quark (see Fig.1). The distributions of events $dN^{event}/dM_{inv}/5$ GeV expected in each bin of 5 GeV versus the invariant mass $M_{inv}(b, 2 quarks_W)$ of the parent three quarks as well as the invariant mass of jets produced by these quarks, i.e. $M_{inv}(b - jet, JETS_W)$, are shown for quark and jets levels in the plots **a)** and **b)** of Fig.5, respectively, for integrated luminosity of $1000 fb^{-1}$.

The distributions of Fig.5 show that the peak positions at quark level (plot **a)**) as well as at jet level (plot **b)**), practically coincide to a good accuracy as well as with the input value of the top quark mass $M_{top} = 170.9(\pm 1.8)$ GeV.

It is also seen from the plot **b)** of Fig.5 that the quark hadronisation into jets leads to a broadening of very small tails which are seen in the invariant mass distribution at quark level (plot **a)** of Fig.5). The right tail is a bit lower and longer than the left one. One may say that the peak picture at jet level still looks more or less symmetric. The main message from these plots is that the appearance of tails due to quark fragmentation into jets does not change the position of the distribution peak, which allows us to reconstruct the input top mass both at quark and jet level.

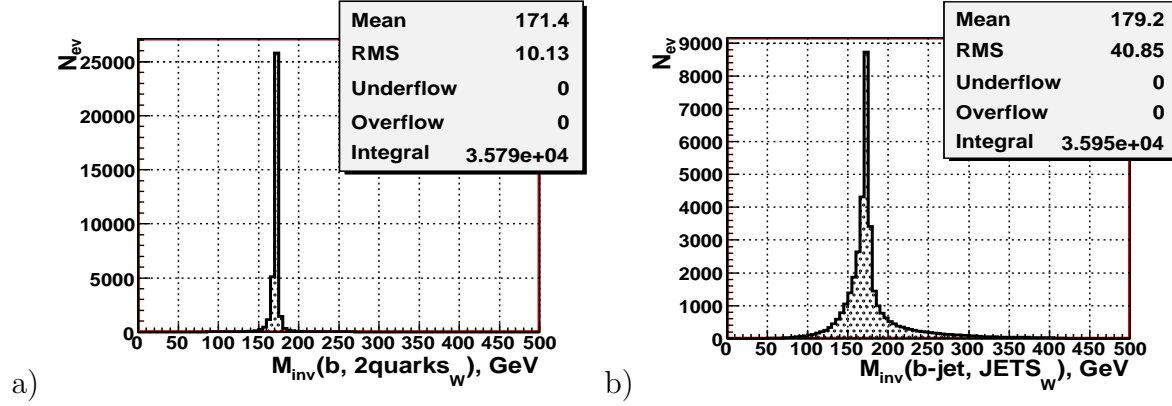


Figure 5: *The top pair production spectra of the invariant masses $M_{inv}(b\text{-jet}, JETS_W)$ of the "b-jet+(all- non-b-jets)" system. **a)** at quark level, **b)** at jet level.*

4 Cuts for the reconstruction of the stop mass.

Based on the results of the previous Section we will use the following three cuts to separate the signal and background:

- there must be at least two b -jets in an event:

$$N_{b\text{-jets}} \geq 2; \quad (14)$$

- the invariant missing mass must be larger than 250 GeV:

$$M_{miss} \geq 250 \text{ GeV}; \quad (15)$$

- the invariant mass of all jets must be smaller than 160 GeV:

$$M_{inv}(Alljets) \leq 160 \text{ GeV}. \quad (16)$$

They reduce the number of top background events from $3.5 \cdot 10^4$ to 12 and leave 1806 stop events. So, the cuts improve the signal-to-background ratio from $S/B = 0.066$ to $S/B \approx 143$ losing about 24% of the signal stop events. The efficiency values for the cuts (14)–(16) are calculated for $\sqrt{s} = 500$ GeV. We define them as the summary efficiencies. It means that if ε_1 is the efficiency of the first cut (14), ε_{12} is the efficiency of applying the first cut (14) and then second cut (15). Analogously, ε_{123} is the efficiency of the successive application of the cuts (14), (15) and (16). The following results are obtained:

$$\begin{aligned} \text{For SIGNAL STOP events:} & \quad \varepsilon_1 = 0.84; \quad \varepsilon_{12} = 0.78; \quad \varepsilon_{123} = 0.76; \\ \text{For BACKGROUND TOP events :} & \quad \varepsilon_1 = 0.94; \quad \varepsilon_{12} = 0.001; \quad \varepsilon_{123} = 3.5 \cdot 10^{-4}. \end{aligned}$$

The distribution of the invariant mass of the "b-jet+(all-non-b-jets)" system in the case of stop pair production is shown in Fig.6. The plots of this figure are analogous to the corresponding plots of Fig.5 using only those stop events that have passed the cuts (14)–(16).

In the stop case, one has to take into account that one of the stops decays into three jets plus a neutralino $\tilde{\chi}_1^0$. Therefore, the right edge of the peak of invariant mass distribution of the "b-jet+($JETS_{W^*}$)" system corresponds to the mass difference $M_{\tilde{t}_1} - M_{\tilde{\chi}_1^0}$. The position of the right edge of the peak $M_{inv}(b\text{-jet}, JETS_{W^*}) \approx 85$ GeV (plot **b**) of Fig.6) coincides with the peak position seen at quark level (plot **a**) of Fig.6). Let us note that the observed

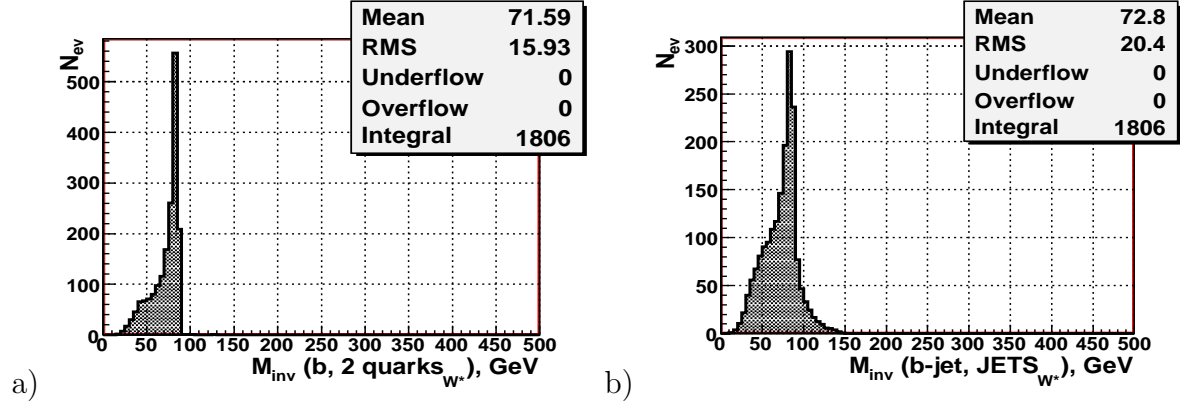


Figure 6: *The spectra of the stop signal events after cuts versus the invariant mass $M_{inv}(b\text{-jet}, JETS_{W^*})$: a) at quark level, b) at jet level. W^* means virtual nature of W boson.*

stability of the peak position in both plots of Fig.6 is due to the rather moderate loss of the number of events that form this peak (they change from ≈ 550 to ≈ 280) while passing from quark level to jet level. Adding the mass of the neutralino $M_{\tilde{\chi}_1^0} = 80.9$ GeV one gets the reconstructed stop mass $M_{\tilde{t}_1}^{reco} \approx 166$ GeV which reproduces well (within bin width of 5 GeV) the input value $M_{\tilde{t}_1} = 167.9$ GeV.

The simulation has shown that the 12 background events are mostly distributed in the region $40 \leq M_{inv}(b\text{-jet}, JETS_W) \leq 140$ GeV, which is 20 times wider than the 5 GeV width of the peak which contains about 280 signal stop events left after the cuts. Therefore, we expect that in future measurements the contribution of a few remaining top background events will not influence the position of this peak which allows one to reconstruct the input value of the stop mass by adding the mass of the neutralino.

The origin of the left tail of the distribution shown in the plot a) of Fig.6 can be clarified by the results of the stop mass reconstruction by calculating its invariant mass at quark level $M_{inv}(b, 2 \text{ quarks}_{W^*}, \tilde{\chi}_1^0)$ as the modulus of the sum of the 4-momenta of all three quarks and the neutralino (see Fig.1) produced in stop decay. These results are given in the plot a) of Fig.7 which shows a very precise reconstruction of the input stop mass at quark level withing the 5 GeV width of a peak.

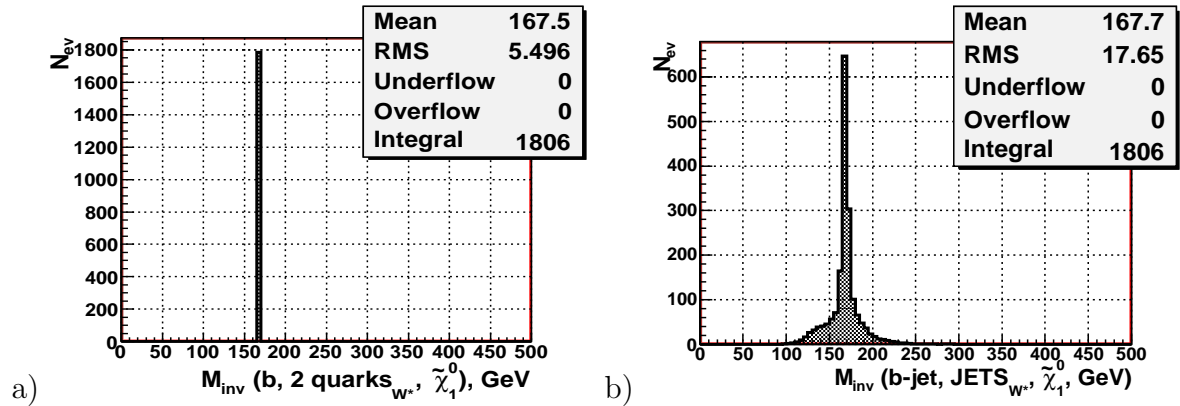


Figure 7: *The spectra of the stop signal events after cuts versus the invariant mass $M_{inv}(b\text{-jet}, JETS_{W^*}, \tilde{\chi}_1^0)$ a) at quark level b) at jet level.*

Comparing the plot a) of Fig.6 with the plot a) of Fig.7 one can conclude that the long left tail as well as the very small right tail in the distribution of $M_{inv}(b, 2 \text{ quarks}_{W^*})$ are caused by the fact that the neutralino 4-momentum is not included in the "b-jet+(all-non-b-jets)"

system. Analogously, comparing plots **b)** and **a)** of Fig.6 one may estimate the contribution of the hadronisation effect (in addition to the contribution of the neutralino momentum) to the left tail of the distribution **b)** in Fig.6.

The influence of the effect of the hadronisation of the b -quarks and of the quarks from W decay into jets is shown in the plot **b)** of Fig.7. It is seen that the hadronisation of quarks into jets does not change the position of the stop mass peak, which still includes the input value $M_{\tilde{t}_1} = 167.9$ GeV, but more or less symmetrical and rather suppressed short tails appear around the peak position. The shape of the peak in the stop plot **b)** Fig.7 looks very similar to the shape of the peak in the top plot **b)** of Fig.5, which demonstrates the stability of the reconstructed top mass peak position after taking into account the effect of quark fragmentation.

4.1 Separation of signal and fake muons.

To select the signal stop pair production events shown in the left plot of Fig.1, one has to identify the muon from the W decay. The distribution of the energy of the signal muons E_{sig-mu} , obtained from the sample of events generated without any cuts, is shown in Fig.8 **a)**. There are, however, also muons in the event coming from leptonic and semileptonic decays of

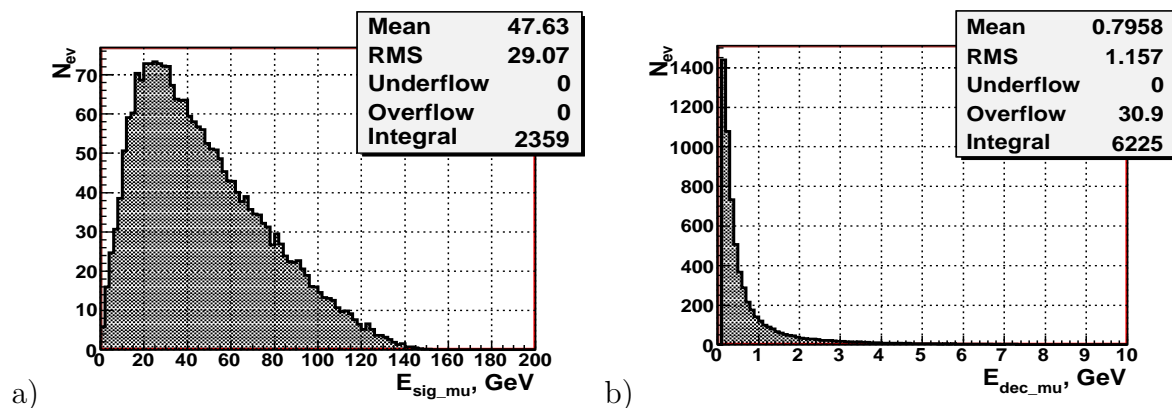


Figure 8: **a)** Energy distribution of signal muons. **b)** Energy distributions of fake muons.

hadrons. Fig.8 **b)** shows the energy E_{dec-mu} of these muons stemming from hadron decays within the detector volume (for which we took the size from [3], [4]). It can be seen that the decay muons have a rather small energy E_{dec-mu} . Its mean value is about 0.81 GeV. The analogous spectrum for the signal muons in Fig.8 **a)** shows that the signal muons have a much higher energy. The mean value E_{sig-mu} is about 50 times higher than the mean value of the energy of the decay muons. One can cut off most low-energy decay muons rejecting those with $E_{mu} \leq 4$ GeV. It leads to a loss of about 15 signal events as seen from the plot **a)** of Fig.8 (the bin in this plot is 2 GeV).

We have also studied another way to select the signal muon from W decay. If the axes of all four jets in the event are known, then in general the signal muon has the largest transverse momentum with respect to any of these jet axes.

4.2 Signal and background cross sections.

We give in Table 1 (without cuts) and Table 2 (after the cuts) the cross sections and the numbers of events for stop pair production and top pair production for five energies \sqrt{s} . To

estimate the rates of stop production at different energies we take the universal value of the luminosity of 1000 fb^{-1} for all energies.

It is seen that the fixed cuts (14)-(16) lead to a strong (more than 3 orders of magnitude) suppression of background top contribution and a moderate loss of signal stop events produced in the energy range $400 \leq \sqrt{s} \leq 800 \text{ GeV}$.

For the stop mass chosen, the largest number of signal events is expected at $\sqrt{s} = 500 \text{ GeV}$. Let us note that, according to [18], a 50% efficiency of the separation of b jets and 80% of the corresponding purity can be expected. It means that to get 1806 reconstructed signal stop events we will need about 2.5 times higher statistics than that provided by the luminosity 1000 fb^{-1} at $\sqrt{s} = 500 \text{ GeV}$.

It is worth noting that, as seen from Table 2, even with the use of the fixed parameters of the cuts (14)–(16) the number of signal stop events that can pass these cuts grows rapidly with the energy in the region $400 \leq \sqrt{s} \leq 500 \text{ GeV}$ where mass measurements will be done in the first phase. These measurements may allow to enlarge the sample of collected signal events and to perform a precise measurement of the stop mass. The region $500 \leq \sqrt{s} \leq 800 \text{ GeV}$, which be available in the second phase of ILC operation, allows to gain a much higher stop statistics, as seen in Table 2. A complete analysis based on adjusting the parameters of the selection cuts (15)-(16) for each of the above energy intervals will be presented in forthcoming papers.

Table 1: The cross sections and the number of events for stop and top pair production before cuts.

$2E_b = \sqrt{s} \text{ [GeV]}$	$\sigma_{stop}^{e^+e^-} \text{ [fb]}$	N_{stop}^{events}	$\sigma_{top}^{e^+e^-} \text{ [fb]}$	N_{top}^{events}	S/B
350	0.23	233	13.76	13750	0.0169
400	1.34	1347	38.79	38740	0.0347
500	2.37	2378	35.94	35950	0.0661
800	1.89	1809	17.36	17359	0.1042
1000	1.42	1265	11.66	11656	0.1085

Table 2: The same as in Table 1 but after cuts.

$2E_b = \sqrt{s} \text{ [GeV]}$	$\sigma_{stop}^{e^+e^-} \text{ [fb]}$	N_{stop}^{events}	$\sigma_{top}^{e^+e^-} \text{ [fb]}$	N_{top}^{events}	S/B
350	0.0089	8	0	0	BKG = 0
400	0.52	521	$2.32 * 10^{-4}$	0.2	2605
500	1.80	1806	$2.26 * 10^{-2}$	12.6	143
800	0.99	995	$1.08 * 10^{-2}$	10	99
1000	0.41	410	$6.26 * 10^{-3}$	6	69

5 Conclusion.

We have studied stop pair production in electron-positron collisions for a stop mass of 167.9 GeV within the framework of the MSSM for the total energies $2E_b = \sqrt{s} = 350, 400, 500, 800, 1000 \text{ GeV}$. We assume that the stop quark decays dominantly into a chargino and a b quark, $\tilde{t}_1 \rightarrow b\tilde{\chi}_1^\pm$, and the chargino decays into a neutralino and a W boson, $\tilde{\chi}_1^\pm \rightarrow \tilde{\chi}_1^0 W^\pm$, where the W boson is virtual. One of the two W's decays hadronically, $W^+ \rightarrow q\bar{q}$, the other one decays leptonically, $W^- \rightarrow \mu^-\nu$.

We have performed a detailed study based on a Monte Carlo simulation with the program PYTHIA6.4 for $\sqrt{s} = 500$ GeV (at this energy we expect the highest number of the signal events for the chosen stop mass $M_{\tilde{t}_1} = 167.9$ GeV and cuts) and the luminosity 1000 fb^{-1} . The program CIRCE1 is used to get the spectra of electron (positron) beams taking into account the effects of beamstrahlung. PYTHIA6.4 is used to simulate stop pair production and decay as well as top pair production being the main background.

Three cuts (14)-(16) for the signal stop events have been proposed to separate signal stop events and top background events. For $\sqrt{s} = 500$ GeV and the luminosity 1000 fb^{-1} they give 1806 signal stop events with 12 top background events. This is different from the more complicated situation in stop pair production at LHC (see, for instance, [17]).

We have shown that the determination of the peak position of the distribution of the invariant mass $M_{inv}(b\text{-jet}, JETS_{W^*})$ of "b-jet+(all-non-b-jets)" system allows one to measure the mass of the stop quark with a good accuracy based on the statistics corresponding to the luminosity 1000 fb^{-1} . For this the mass of χ_1^0 has to be known.

As seen from the Table 2 the measurements at other energies in the regions $400 \leq \sqrt{s} \leq 500$ GeV and $500 \leq \sqrt{s} \leq 800$ GeV may allow to enlarge substantially the number of selected signal stop events and to perform a precise measurement of the mass of the scalar top quark.

In conclusion we can say that the e^+e^- channel is well suited for the study of stop pair production at ILC.

6 Acknowledgements.

This work is supported by the JINR-BMBF project and by the "Fonds zur Förderung der wissenschaftlichen Forschung" (FWF) of Austria, project No.P18959-N16. The authors acknowledge support from EU under the MRTN-CT-2006-035505 and MRTN-CT-2004-503369 network programmes. A.B. was supported by the Spanish grants SAB 2006-0072, FPA 2005-01269 and FPA 2005-25348-E of the Ministerio de Educacion y Ciencia.

References

- [1] Ellis J. and Rudaz S. // Phys. Lett. B. 1983. V. 128, P. 248,
Altarelli G. and Rückl R. // Phys. Lett. B. 1984. V. 144, P. 126.
- [2] D0 Collab., Abazov V.M. et al. // Phys. Lett. B. 2007. V. 645, P. 119.
CDF Collab., Aaltonen T. et al. // Phys. Rev. D. 2007. V. 76, P. 072010 .
- [3] International Linear Collider, Reference Design Report, V.1 , Executive Summary.
Editors: Brau J., Okada Y., Walker N. // ILC-REPORT-2007-001, August 2007;
<http://www.linearcollider.org/cms/?pid=1000025>.
- [4] International Linear Collider, Reference Design Report, V. 2, Physics at the ILC.
Editors: Djouadi A., Lykken J., Mönig K., Okada Y., Oreglia M., Yamashita S. // ILC-REPORT-2007-001, August 2007 ; arXiv:0709.1893 [hep-ph];
<http://www.linearcollider.org/cms/?pid=1000025>.
- [5] Bartl A., Mönig K., Majerotto W., Skachkova A.N., Skachkov N.B.
Pair Production of Scalar Top Quarks in e^+e^- Collisions at ILC // ILC-NOTE-2007-036,
arXiv:0804.2125[hep-ph].

- [6] Bartl A., Mönig K., W.Majerotto W., Skachkova A.N., Skachkov N.B.
Pair Production of Scalar Top Quarks in Polarized Photon-Photon Collisions at ILC // ILC-NOTE-2007-036, arXiv:0804.1700[hep-ph].
- [7] Bartl A., Eberl H., Kraml S., Majerotto W. and Prosd W. // Eur. Phys. J. C. 2000. V. 2, P. 6; hep-ph/0002115.
- [8] Bartl A., Moenig K, Majerotto W., Skachkova A.N., Skachkov N.B.
Stop pair production in polarized photon-photon collisions // Proc. of the Intern. Conf. on Linear Colliders (LCWS 2004), April 19-23, 2004, Le Carre des Sciences, Paris, France, 2004. Vol. II, P. 919.
- [9] Carena M. et al. // Phys. Rev. D. 2005 V. 72, P. 115008; hep-ph/0508152.
- [10] Sjöstrand T., Edén P., Friberg C., Lönnblad L., Miu G., Mrenna S. and Norrbin E. // Computer Phys. Commun. 2001. V. 135, P. 238.
- [11] Ohl T. $\kappa\mu\rho\kappa\eta$, Version 1.0: Beam Spectra for Simulating Linear Collider Physics // hep-ph/9607454.
- [12] Gunion J.F. and Haber H.E. // Nucl. Phys. B. 1986. V. 272, P. 1; Nucl.Phys. B. 1986. V. 278, P. 449; Erratum. Nucl. Phys. B. 1993. V. 402, P. 567.
- [13] Brubaker E. et al. Combination of CDF and D0 results on the mass of the top quark; By Tevatron Electroweak Working Group // Fermilab-TM-2380-E. 2007. arXiv:hep-ex/0703034.
- [14] Moortgat-Pick G. et al. The role of polarized positrons and electrons in revealing fundamental interactions at the Linear Collider // hep-ph/0507011.
- [15] Yokoya K. and Chen P. Beam-beam phenomena in linear colliders // KEK Preprint 91-2, April 1991.
Shulte D., Ph.D. thesis
http://www.sldnt.slac.stanford.edu/nlc/programs/guinea_pig/gp_index.html.
- [16] Hawkings R. Vertex detector and flavour tagging studies for TESLA linear collider // LC-PHSM-2000-021, 2000.
- [17] Dydak U. Search for the stop quark with CMS at the LHC // CMS TN/96-022, CERN, 1996.
Dydak U., Rohringer H. and Tuominiemi J. Study of the channel gluino \rightarrow stop + top // CMS TN/96-103. CERN. 1996.
- [18] Damerell C.J.S, Jackson D.J. // 1996. eConf960625. DET078.
Hawkings R. // 2000. LC-PHSM-2000-021.
Xella Hansen S.M., Jackson D.J., Hawkings R., Damerell C.J.S. // 2001. LC-PHSM-2001-024.
Xella Hansen S.M., Wing M., Jackson D.J., De Groot N., Damerell C.J.S. // 2003. LC-PHSM-2003-061.
Xella Hansen S.M. et al. [Linear Collider Flavour Identification Collaboration] // Nucl. Instrum. Meth. A. 2003. V. 501, P. 106.
Hillert S., Damerell C.J.S. // 2005. eConf0508141. ALCPG 1403.